Chemical Science

ROYAL SOCIETY OF CHEMISTRY

EDGE ARTICLE

View Article Online
View Journal | View Issue

Cite this: *Chem. Sci.*, 2022, **13**, 8060

All publication charges for this article have been paid for by the Royal Society of Chemistry

Received 15th May 2022
Accepted 7th June 2022

DOI: 10.1039/d2sc02698h

rsc.li/chemical-science

Switchable photocatalysis for the chemodivergent benzylation of 4-cyanopyridines†

Eleni Georgiou,‡[ab] Davide Spinnato,‡[ab] Kang Chen,[a] Paolo Melchiorre *[ac] and Kilian Muñiz§

We report a photocatalytic strategy for the chemodivergent radical benzylation of 4-cyanopyridines. The chemistry uses a single photoredox catalyst to generate benzyl radicals upon N–F bond activation of 2-alkyl *N*-fluorobenzamides. The judicious choice of different photocatalyst quenchers allowed us to select at will between mechanistically divergent processes. The two reaction manifolds, an *ipso*-substitution path proceeding *via* radical coupling and a Minisci-type addition, enabled selective access to regioisomeric C4 or C2 benzylated pyridines, respectively. Mechanistic investigations shed light on the origin of the chemoselectivity switch.

Introduction

Pyridines and related nitrogen heterocycles are prevalent in pharmaceuticals and agrochemicals,[1] so methods are needed for their regioselective functionalization. The recent resurgence of photoredox catalysis[2] and electrochemistry[3] has triggered the development of new pyridine functionalization strategies based on radical pathways. One such approach exploits the unique reactivity of 4-cyanopyridines **1** (Fig. 1a), which are prone to single-electron transfer (SET) reduction to form kinetically stable dearomatized radical anions **I** (path i). These open-shell intermediates **I** can then couple with other radicals offering, upon cyanide extrusion, a selective *ipso*-substitution manifold to access C4-functionalized pyridines.[4] The venerable Minisci reaction[5] is another effective approach for the functionalization of pyridines, which is based on the addition of nucleophilic carbon radicals onto protonated heteroaromatic compounds. Due to their decreased π-electron density, 4-cyanopyridines generally participate in Minisci-type functionalization with C2 regioselectivity (path ii in Fig. 1a).[6]

In this manuscript, we describe the development of switchable photocatalytic methods[7] that allowed us to select at will between the functionalization of 4-cyanopyridines at the C4 or C2 position, leading to products **3** and **4** respectively (Fig. 1b).

Specifically, we used a single photoredox catalyst to activate, *via* an SET reduction, the N–F bond within 2-alkyl *N*-fluorobenzamides **2**.[8] A 1,5-hydrogen atom transfer (1,5-HAT), mastered by the resulting amidyl radical **II**, then afforded the benzylic radical **III**. We serendipitously observed that different photocatalyst quenchers enabled mechanistically divergent processes, triggering either an *ipso*-substitution (path i) or a Minisci manifold (path ii). This additive-controlled mechanistic switch afforded benzylated pyridines **3** and **4** with different regioselectivity. Considering the paucity of methods available for the benzylation of pyridines,[9] and the ability of controlling the chemoselectivity to dictate the regio-isomeric outcome of the process by simply changing additives, we decided that a detailed investigation was worth pursuing.

Design plan

This study was prompted by the interest of the late Kilian Muñiz in the activation of *N*-halogenated compounds to form the corresponding *N*-centered radicals, and their use in 1,5-HAT to initiate position-selective C(sp^3)–H functionalization reactions.[10] The original plan (Fig. 2a) was to use a photoredox catalyst (**PC**) to activate, *via* an SET reduction, the N–F bond within *N*-(*tert*-butyl)-*N*-fluoro-2-methylbenzamide (**2a**, E_{red} = −0.84 V *vs.* SCE).[8a] By triggering the sequence detailed in Fig. 1b, this SET would afford the benzyl radical **III**. Engaging **III** in an *ipso*-substitution manifold would also require the SET reduction of 4-cyanopyridine **1a** (E_{red} = −1.60 V *vs.* SCE)[11] to form the radical anion **I**. We surmised that the activation of **1a** could also be mastered by **PC**. Crucial for the sequential activation of substrates **1** and **2** would be therefore a donor additive capable of efficiently turning over the photocatalyst **PC** by facilitating SET reduction of the oxidized $\mathbf{PC}^{+\cdot}$.

[a]*ICIQ – Institute of Chemical Research of Catalonia, The Barcelona Institute of Science and Technology, Avenida Països Catalans 16 – 43007, Tarragona, Spain. E-mail: pmelchiorre@iciq.es; Web: https://www.iciq.org/research/research_group/prof-paolo-melchiorre*

[b]*Department of Analytical Chemistry and Organic Chemistry, University Rovira i Virgili (URV), 43007, Tarragona, Spain*

[c]*ICREA, Passeig Lluís Companys 23 – 08010, Barcelona, Spain*

† Electronic supplementary information (ESI) available: Experimental procedures, full characterization data, and copies of NMR spectra (PDF). See https://doi.org/10.1039/d2sc02698h

‡ These authors contributed equally to this work.

§ Prof. Dr Kilian Muñiz: deceased, March 16, 2020.

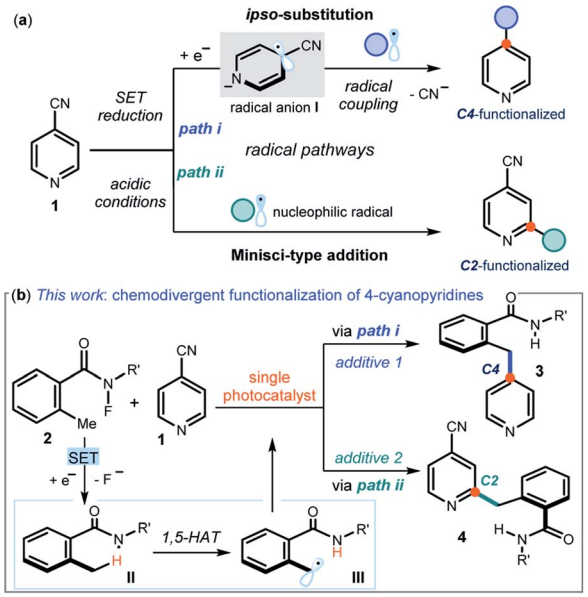

Fig. 1 (a) Radical pathways available for the functionalization of 4-cyanopyridines. (b) A photoredox system that uses different additives to switch between different mechanisms to afford C4 or C2 benzylated products **3** or **4** at will.

Results and discussion

The feasibility of our plan was tested by selecting 1,3-dicyano-2,4,5,6-tetrakis(diphenylamino)-benzene **A** as photocatalyst (see Section E1 in the ESI† for the screening of other photoredox catalysts). This choice was informed by the redox potential of **A** ($E_{1/2}(\mathbf{A}^+/\mathbf{A}^*) = -1.52$ *vs.* SCE),[12] which makes it potentially suitable for activation of both **1a** and **2a** *via* SET reduction.[13] Initial experiments were conducted in 1,2-dichloroethane (DCE) using a blue LED emitting at 465 nm (Fig. 2b). The choice of the donor additives (3 equiv.), which served as reductive quenchers of **A**, was critical for efficiency. Tertiary amines, including DIPEA (*N*,*N*-diisopropylethylamine) and pentamethyl piperidine (N–Me TMP), smoothly afforded the *ipso*-benzylated product **3a** (entries 1–2), with DIPEA offering the best yield (75%, entry 1). A strained bicyclic amine (DABCO) was not suitable for this process (entry 3). Surprisingly, non-basic quenchers completely switched the reaction manifold towards a Minisci pathway, leading exclusively to the formation of the C2 benzylated pyridine **4a**. Specifically, triphenylphosphine (PPh_3), Hantzsch ester (HE), and γ-terpinene all channeled the radical process towards a C2-selective pattern (entries 4–6). Further optimization using PPh_3 as the quencher established that H_2O (5 equiv., entry 7) improved the yield of **4a** to 60%. Performing the process under air completely suppressed the *ipso*-substitution manifold, while the Minisci-type reaction remained unaffected (entries 8–9). Control experiments indicated that the reductive quencher (entry 10), the photocatalyst, and light irradiation were necessary for reactivity.

Investigations were then performed to gain insight into the origin of the mechanistic switch. Since Minisci reactions require acidic conditions[5] for effective heteroarene activation, we measured the pH of the two reaction systems by means of a pH meter (see Fig. 2c and Section F in the ESI† for details). The C2 selective system, mastered by PPh_3, had a pH of 3.1, which is suitable for a Minisci pathway. In contrast, we measured a pH of 9.8 for the DIPEA-based protocol, leading to the *ipso*-substitution product **3a**. This observation hints to the acidity of the reaction medium as responsible for channeling the process towards different mechanistic paths. A basic quencher (DIPEA) ensures photocatalyst **A** turnover while keeping a basic pH by neutralizing the HCN and HF generated upon SET activation of substrates **1a** and **2a**, respectively. Switching to neutral

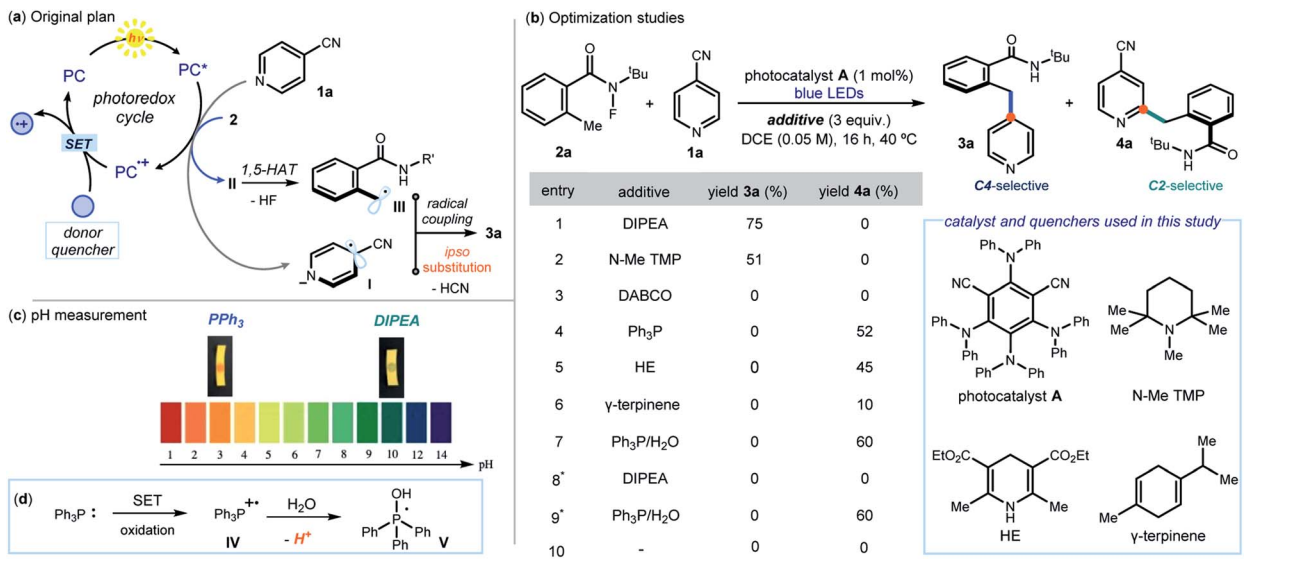

Fig. 2 Initial explorations. (a) Design plan. (b) Optimization studies: reactions performed under argon on a 0.1 mmol scale at 40 °C for 16 h under illumination by a blue LED strip (λ_{max} = 465 nm, 14 W) using 3 equiv. of **1a** and additive. Yield determined by ^{1}H NMR analysis. (c) Measuring the pH of the reaction media. (d) Rationale for the acidity increase in the PPh_3-based protocol. *Performed under air.

quenchers (PPh_3, but also HE and γ-terpinene, entries 4–6 in Fig. 2b) avoids the possibility of buffering the build-up of acidity. In addition, the possible SET oxidation of PPh_3 ($E_{1/2}$ = +0.98 V *vs.* SCE) from the photocatalyst would afford the radical cation **IV**, which is known to deliver the phosphoranyl radical **V** liberating protons upon addition of water (Fig. 2d).[14] Overall, the PPh_3-based protocol ensures the acidic conditions needed for an effective Minisci pathway, which overrides the *ipso*-substitution manifold. This scenario is congruent with kinetic profile analyses of the two systems, detailed in Section I of the ESI,† that established the Minisci C2-selective path to proceed faster than the C4-selective process (after 75 minutes, the Minisci product is formed in 60% yield, while the *ipso*-substitution adduct in about 5% yield). The Minisci pathway also showed an induction period, which was suppressed upon addition of TFA (5 mol%). This reactivity profile is coherent with the need for the reaction medium's pH to be low enough to switch on the Minisci pathway.[13] Importantly, the Minisci reaction cannot be promoted by simple addition of stoichiometric amounts of TFA and removal of PPh_3 (see Section E2, Table S3, entry 12–13 in the ESI†). This indicates the unique ability of the neutral quencher to switch on an effective photocatalytic pathway that enables the C2-selective process.

After delineating a rationale for the observed chemodivergency, we explored the synthetic applicability of our photocatalytic systems by adopting the optimized conditions in entries 1 and 7 of Fig. 2b. Both protocols required the same reaction conditions (substrates, photocatalyst **A**, and solvent),

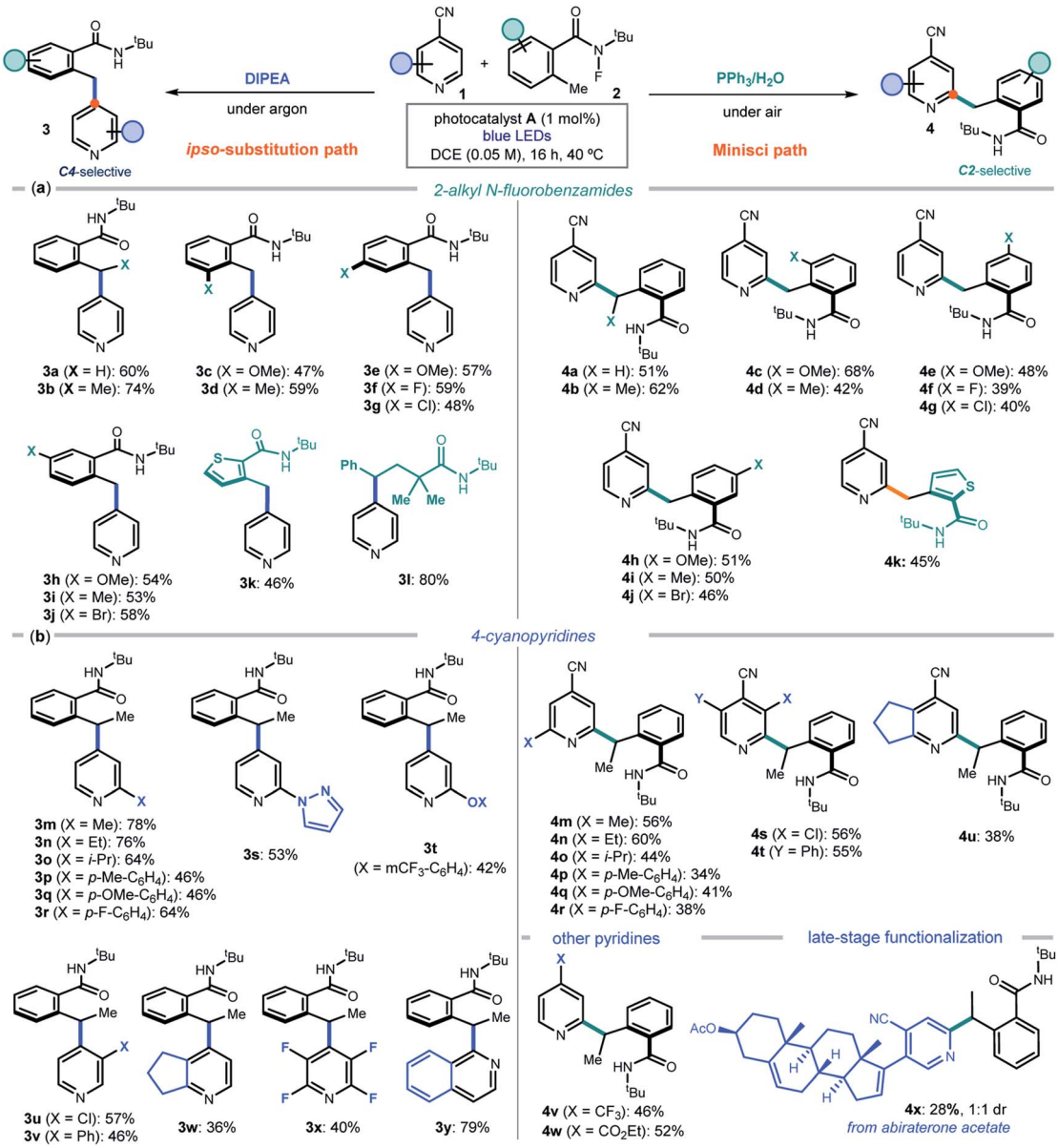

Fig. 3 Switchable photocatalytic strategy for the chemodivergent C4 and C2 radical benzylation of 4-cyanopyridines. Survey of the (a) *N*-fluoroamides **2** and (b) 4-cyanopyridines **1** that can participate in the processes. Reactions performed using 3 equiv. of **1** and 3 equiv. of additive; yields refer to isolated products **3** and **4** after purification.

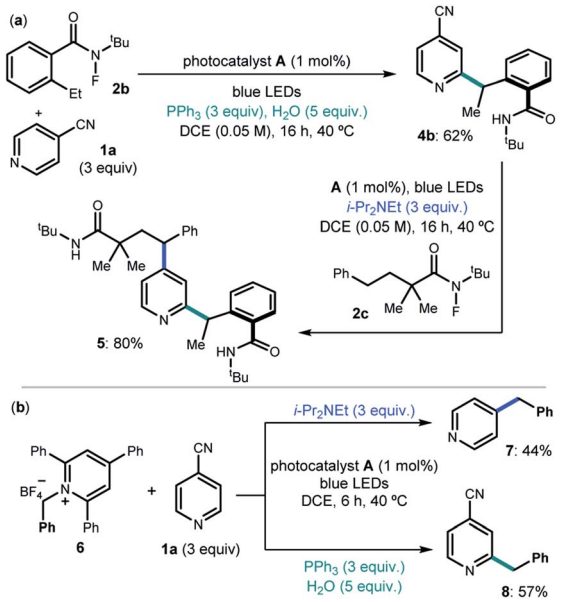

Scheme 1 (a) Sequential procedure for the difunctionalization of 4-cyanopyridine **1a**. (b) *Ipso*-substitution (C4 selective) and Minisci-type reaction (C2 selective) for the benzylation of **1a** with *N*-benzyl pyridinium **6**.

but differed in the additive used (DIPEA or PPh_3). We first evaluated the 2-alkyl *N*-fluorobenzamides **2** that could participate in the *ipso*-substitution and the Minisci processes with 4-cyanopyridine **1a** leading to C4 or C2 benzylated pyridines **3** and **4**, respectively (Fig. 3a).

A methyl substituent at the benzylic position of **2** was well-tolerated (products **3b** and **4b**), as was the presence of both electron-donating groups and halides at various positions of the aryl ring (adducts **c–j** in both protocols). A heteroaryl moiety, such as a thiophenyl, could be installed in products **3k** and **4k**. The *ipso*-substitution protocol could be extended to include a linear *N*-fluoramide that, upon N–F activation and 1,5-HAT, formed a benzylic radical eventually leading to product **3l**. The linear substrate offered poor reactivity (<20%) in the Minisci protocol. Linear *N*-fluoramides that do not lead to benzylic radicals proved unreactive (a list of unsuccessful and moderately reactive substrates is reported in Fig. S4 of the ESI†).

We then explored the cyanopyridines **1** that could react with 2-ethyl *N*-fluorobenzamide **2b**, applying both C4 and C2-selective protocols (Fig. 3b). Various substituents were tolerated at the pyridine 2-position, leading to products **3m–r** and **4m–r**. A fused cyclopentane substrate provided products **3w** and **4u** in moderate yield. Focusing on the *ipso*-substitution pathway, we found that a pyrazole and a phenol ether substituent could be successfully installed in pyridines **3s** and **3t**. Moreover, 3-substituted cyanopyridines and 2,3,5,6-tetrafluoro-4-cyanopyrine also reacted smoothly, leading to products **3u–v** and **3x**, respectively. A different heteroarene scaffold, such as 1-cyanoquinoline, afforded the *ipso*-substitution product **3y** in high yield. As for the C2-selective Minisci protocol, substitution at the 3-position of the cyanopyridines was tolerated, with a chloro substituent affording the more crowded regioisomer **4s** (halogens at the C3 position act as *ortho*-activators)[5d] while the sterically hindered phenyl group leading to adduct **4t**. 4-Substituted pyridines bearing electron-withdrawing groups other than nitrile, including a trifluoromethyl and an ester, afforded **4v** and **4w** in good yields. The Minisci-type addition was also suitable for the direct functionalization of a biorelevant compound, since abiraterone acetate (a medication used to treat prostate cancer) was successfully benzylated, leading to adduct **4x** in satisfactory yield.

We then considered the development of a sequential protocol for the difunctionalization of pyridines (Scheme 1a). Capitalizing on the pH-regulated switchable methods, we first conducted the Ph_3P-enabled Minisci process to couple 4-cyanopyridine **1a** and 2-ethyl *N*-fluorobenzamide **2b** with C2-selectivity. The resulting product **4b**, upon isolation, was reacted with the linear *N*-fluoroamide **2c** using DIPEA to select the C4-selective *ipso*-substitution manifold. The overall sequence smoothly delivered the complex pyrdine **5**.

We also investigated if the generality of our chemodivergent system could be expanded to include different radical precursors (Scheme 1b). Specifically, the pyridinium salt **6**, which is prone to facile SET reduction ($E_{red} = -1.01$ V *vs.* Ag/AgCl),[15] was successfully activated towards benzyl radical formation in both systems, delivering C2 and C4 benzylated pyridines **7** and **8** in satisfactory yields.

Conclusions

In summary, we have developed a photoredox strategy that allows switchable control of the chemoselectivity in the radical benzylation of 4-cyanopyridines. An *ipso*-substitution path leads to C4 benzylated pyridines, while a Minisci-type addition affords products with C2 selectivity. The two reactivity manifolds, which require the same photoredox catalyst, reaction conditions, and substrates, are selected at will by the choice of the photocatalyst quencher. The switchable photocatalytic system was successfully applied with two different benzylic radical precursors. Mechanistic studies established that a change in the reaction medium's pH is responsible for channeling the process towards chemodivergent pathways.

Data availability

Electronic supplementary information (ESI†) available: details of experimental procedures, full characterization data, and copies of NMR spectra (PDF).

Author contributions

E. G., D. S., and K. C. performed the experiments. K. M. was involved in the conceptualization of the process. P. M. directed the project. P. M. wrote the manuscript with assistance from all authors. E. G. and D. S. contributed equally to this work.

Conflicts of interest

There are no conflicts to declare.

Acknowledgements

Financial support was provided by Agencia Estatal de Investigación (PID2019-106278GB-I00 to PM and CTQ2017-88496-R to KM) and the MCIN/AEI/10.13039/501100011033 (CEX2019-000925-S). E.G. thanks MINECO (CTQ2017-88158-R) for a predoctoral fellowship. The authors thank Dr Will C. Hartley (ICIQ) for insightful discussions.

Notes and references

1 E. Vitaku, D. T. Smith and J. T. J. Njardarson, *J. Med. Chem.*, 2014, **57**, 10257–10274.

2 (*a*) P. Melchiorre, *Chem. Rev.*, 2022, **122**, 1483–1484, and reviews cited therein.; (*b*) M. H. Shaw, J. Twilton and D. W. C. MacMillan, *J. Org. Chem.*, 2016, **81**, 6898–6926.

3 M. Yan, Y. Kawamata and P. S. Baran, *Chem. Rev.*, 2017, **117**, 13230–13319.

4 For a review:(*a*) S. Tong, K. Li, X. Ouyang, R. Song and J. Li, *Green Synth. Catal.*, 2021, **2**, 145–155For seminal examples:(*b*) T. Caronna, A. Clerici, D. Coggiola and S. Morrocchi, *Tetrahedron Lett.*, 1981, **22**, 2115–2118; (*c*) R. Bernardi, T. Caronna, S. Morrocchi and M. Ursini, *J. Heterocyclic Chem.*, 1996, **33**, 1137–1142For selected recent examples:(*d*) A. McNally, C. K. Prier and D. W. C. MacMillan, *Science*, 2011, **334**, 1114–1117; (*e*) M. T. Pirnot, D. A. Rankic, D. B. C. Martin and D. W. C. MacMillan, *Science*, 2013, **339**, 1593–1596; (*f*) T. Hoshikawa and M. Inoue, *Chem. Sci.*, 2013, **4**, 3118–3123.

5 For a review:(*a*) R. S. J. Proctor and R. J. Phipps, *Angew. Chem., Int. Ed.*, 2019, **58**, 13666–13699 and references therein.For seminal reports:(*b*) F. Minisci, R. Bernardi, F. Bertini, R. Galli and M. Perchinummo, *Tetrahedron*, 1971, **27**, 3575–3580; (*c*) F. Minisci, F. Fontana and E. Vismara, *J. Heterocycl. Chem.*, 1990, **27**, 79For recent selected examples:(*d*) F. O'Hara, D. G. Blackmond and P. S. Baran, *J. Am. Chem. Soc.*, 2013, **135**, 12122–12134; (*e*) A. Gutiérrez-Bonet, C. Remeur, J. K. Matsui and G. A. Molander, *J. Am. Chem. Soc.*, 2017, **139**, 12251–12258; (*f*) J. Jin and D. W. C. MacMillan, *Angew. Chem., Int. Ed.*, 2015, **54**, 1565–1569.

6 (*a*) A. Nikolaev, C. Y. Legault, M. Zhang and A. Orellana, *Org. Lett.*, 2018, **20**, 796–799; (*b*) X. Li, H.-Y. Wang and Z.-J. Shi, *New J. Chem.*, 2013, **37**, 1704–1706.

7 Y. Sakakibara and K. Murakami, *ACS Catal.*, 2022, **12**, 1857–1878 and references therein.

8 (*a*) Q. Guo, Q. Peng, H. Chai, Y. Huo, S. Wang and Z. Xu, *Nat. Commun.*, 2020, **11**, 1463–1472For metal-catalyzed N-F bond activation protocols, see:(*b*) B. J. Groendyke, D. I. AbuSalim and S. P. Cook, *J. Am. Chem. Soc.*, 2016, **138**, 12771–12774; (*c*) Z. Li, Q. Wang and J. Zhu, *Angew. Chem., Int. Ed.*, 2018, **57**, 13288–13292; (*d*) Z. Zhang, L. H. Stateman and D. A. Nagib, *Chem. Sci.*, 2019, **10**, 1207–1211; (*e*) Q.-Q. Min, W.-Y. Shi, Z. Zhang and Y.-M. Liang, *Org. Lett.*, 2021, **23**, 2693–2698; (*f*) D. Bafaluy, J. M. Muñoz-Molina, I. Funes-Ardoiz, S. Herold, A. J. de Aguirre, G. Zhang, F. Maseras, T. R. Belderrain, P. J. Pérez and K. Muñiz, *Angew. Chem., Int. Ed.*, 2019, **58**, 8912–8916.

9 For *ipso*-benzylation:(*a*) B. M. Vittimberga, F. Minisci and S. Morrocchi, *J. Am. Chem. Soc.*, 1975, **97**, 4397–4398For Minisci-type processes:(*b*) M. Wan, H. Lou and L. Liu, *Chem. Commun.*, 2015, **51**, 13953–13956.

10 (*a*) C. Martinez and K. Muñiz, *Angew. Chem., Int. Ed.*, 2015, **54**, 8287–8291; (*b*) A. E. Bosnidou, T. Duhamel and K. Muñiz, *Eur. J. Org. Chem.*, 2020, 6361–6365 and references therein. See also Ref. 8f.

11 M. C. Nicastri, D. Lehnherr, Y.-H. Lam, D. A. DiRocco and T. Rovis, *J. Am. Chem. Soc.*, 2020, **142**, 987–998.

12 M. Garreau, F. Le Vaillant and J. Waser, *Angew. Chem., Int. Ed.*, 2019, **58**, 8182–8186.

13 The simplistic mechanistic picture detailed in Fig. 2a, based on the SET reduction of **1a** and **2a** by photocatalyst **A**, served as our initial design plan. Detailed investigations, including quantum yield determination, Stern–Volmer quenching studies, and cyclic voltammetry, suggested a more complex mechanistic scenario for both protocols based on a reductive quenching cycle, which is discussed in Section G of the ESI†

14 (*a*) G. Pandey, D. Pooranchand and U. T. Bhalerao, *Tetrahedron*, 1991, **47**, 1745–1752; (*b*) Y. Masuda, H. Tsuda and M. Murakami, *Angew. Chem., Int. Ed.*, 2021, **60**, 3551–3555.

15 M. Ociepa, J. Turkowska and D. Gryko, *ACS Catal.*, 2018, **8**, 11362–11367.